Analytical Cellular Pathology 35 (2012) 395–405
DOI 10.3233/ACP-2012-0068
IOS Press

Fluorescence *in situ* hybridization (FISH) signal analysis using automated generated projection images

Xingwei Wang[a], Xiaodong Chen[b], Yuhua Li[b], Hong Liu[b,*], Shibo Li[c], Roy R. Zhang[c] and Bin Zheng[a]
[a]*Department of Radiology, University of Pittsburgh, Pittsburgh, PA, USA*
[b]*Department of Electrical and Computer Engineering, University of Oklahoma, Norman, OK, USA*
[c]*Department of Pediatrics, University of Oklahoma Health Sciences Center, Oklahoma, OK, USA*

Received: 14 January 2012
Accepted: 24 July 2012

Abstract. Fluorescence *in situ* hybridization (FISH) tests provide promising molecular imaging biomarkers to more accurately and reliably detect and diagnose cancers and genetic disorders. Since current manual FISH signal analysis is low-efficient and inconsistent, which limits its clinical utility, developing automated FISH image scanning systems and computer-aided detection (CAD) schemes has been attracting research interests. To acquire high-resolution FISH images in a multi-spectral scanning mode, a huge amount of image data with the stack of the multiple three-dimensional (3-D) image slices is generated from a single specimen. Automated preprocessing these scanned images to eliminate the non-useful and redundant data is important to make the automated FISH tests acceptable in clinical applications. In this study, a dual-detector fluorescence image scanning system was applied to scan four specimen slides with FISH-probed chromosome X. A CAD scheme was developed to detect analyzable interphase cells and map the multiple imaging slices recorded FISH-probed signals into the 2-D projection images. CAD scheme was then applied to each projection image to detect analyzable interphase cells using an adaptive multiple-threshold algorithm, identify FISH-probed signals using a top-hat transform, and compute the ratios between the normal and abnormal cells. To assess CAD performance, the FISH-probed signals were also independently visually detected by an observer. The Kappa coefficients for agreement between CAD and observer ranged from 0.69 to 1.0 in detecting/counting FISH signal spots in four testing samples. The study demonstrated the feasibility of automated FISH signal analysis that applying a CAD scheme to the automated generated 2-D projection images.

Keywords: Fluorescence *in situ* hybridization (FISH), automated FISH signal analysis, computer-aided detection (CAD), molecular imaging biomarker

1. Introduction

Fluorescence *in situ* hybridization (FISH) tests provide molecular imaging biomarkers that have been expansively studied as promising imaging tools to improve the accuracy in cancer diagnosis and its prognosis assessment [1, 2]. Studies have shown that FISH provided a higher statistical accuracy and discriminatory power than the conventional karyotyping method in cancer detection and diagnosis [3, 4]. Specifically, FISH test is able to discover cryptic abnormalities and identify structural/numerical abnormalities that may be missed by conventional cytogenetic examinations due to a number of advantages of FISH tests that enable to improve the accuracy and/or consistency in cancer diagnosis by targeting the visualization and detection of specific chromosome changes based on different DNA probes. In addition, although both metaphase and

*Corresponding author: Hong Liu, Department of Electrical and Computer Engineering, University of Oklahoma, 202 West Boyd St. Room 219, Norman, OK 73019, USA. Tel.: +1 405 325 4286; Fax: +1 405 325 7066; E-mail: liu@ou.edu.

interphase based FISH tests can be applied in cancer diagnosis, the interphase cell based FISH imaging and signal analysis is a more efficient and popular detection and diagnostic approach because the culturing of metaphase cells is not required and the number of analyzable interphase cells can be substantially increased. As a result, the interphase FISH tests have been widely investigated and applied to the variety of cancer detection and diagnosis (including breast [5], cervical [6], lung [7], bladder [8], and blood cancer (leukemia) [9] using a variety of FISH-probed cytologic specimens such as fine needle aspirates, effusion, urine, blood, and bone marrow). Due to the advantages of FISH tests, current American Society of Clinical Oncology/College of American Pathologists and National Cancer Institute guidelines have recommended the incorporation of interphase FISH tests to the diagnostic work-up of breast cancer and leukemia patients [10, 11].

To conduct FISH tests, the manual FISH signal detection and analysis method is currently routinely performed in the cytogenetic laboratories. Using a fluorescence microscope and switching between different fluorescent signal band-pass filters, a laboratory technician first visually searches for and selects an analyzable interphase cell with "good" morphology in each FISH-probed sample specimen. Then, he/she visually adjusts microscopic objective lens to focus on the FISH-probed signals and count the number of independent FISH-probed signal spots depicted inside the targeted cell. To minimize the FISH signal counting bias, the technician requires to identifying between 100 and 200 analyzable cells and computes a summary index of the FISH signals based on all examined cells. This manual FISH analysis method has a number of disadvantages. First, it may generate substantial inter-reader variability in disease diagnosis and its prognosis prediction. Up to 24% discordance was reported in previous study [12]. Second, it may introduce the inevitable bias due to the random selection of cells, which reduces the diagnostic sensitivity and specificity in quantifying residual disease in response to therapy, particularly in heterogeneous cases with a high fraction of normal cells in certain local areas [13]. For example, when applying FISH test to assess HER2 status of malignant breast lesions, higher than 20% inaccuracy rate has been reported [10]. Third, it typically takes 30 to 60 minutes for an experienced observer to visually analyze one FISH probed slide [14], which is quite time-consuming. Therefore, manual FISH analysis severely limits its routine clinical utility [15].

To overcome the limitations of manual FISH signal analysis methods, developing automated FISH signal analysis systems and methods has been attracting research interests in the last two decades. As a result, several commercialized fluorescent image scanning systems including but not limited to (1) Ikoniscope fast-FISH imaging system (Ikonisys Inc., New Haven, CT), (2) Metafer4 (MetaSystems, Altlussheim, Germany), (3) Duet system (BioView Ltd, Nes Ziona, Israel), and (4) ScanScope FL (Aperio Inc., Vista, CA, USA) are available and tested by different groups. For example, Netten et al., reported the first automated FISH image analysis system that enables to count FISH signals that are neither split nor stringy in a single spectrum [16]. Since then, several other automated FISH image analysis systems and schemes have been developed and tested [3, 17–19]. In these schemes, different image processing methods, including the user-defined thresholds [3], artificial neural networks [17], the watershed algorithm [19], and the Isodata algorithm [20], were used to segment interphase cell nuclei. Despite the reported encouraging results and progress, none of these automated FISH image analysis methods have been routinely used in cytogenetic laboratories due to both the hardware and software limitations (i.e., the existing commercialized FISH image scanning systems are unable to acquire high-resolution FISH images in a fully-automated image scanning mode and the computerized schemes are unable to accurately distinguish and merge splitting and stringy FISH signals).

In our group, we recently designed and implemented a new FISH image scanning system that enables to acquire high-resolution interphase FISH images under a fully-automated multi-spectral image scanning mode [21]. The primary differences between our FISH image scanning system and the existing commercialized systems are as follows. First, our system is a fully-automated image scanning system to acquire several spectral FISH images simultaneously, while many existing systems require multiple scans by switching the optical fluorescent filters. Second, our system aims to acquire high-resolution FISH images under an image scanning mode, while the most existing systems work on acquisition of low-resolution images in a scanning mode and then acquisition of high-resolution images in a still image mode. Third, our system uses a multi-spectral imaging approach, while

some of the other systems used a hyper-spectral imaging approach (in particular for those aimed to acquire images of multiplex fluorescence *in-situ* hybridization (M-FISH) images of metaphase chromosomes [22]). Although our approach has advantages, it also has disadvantages. For example, to acquire high-resolution scanning images, our system should have and maintain high magnification power throughout the image scanning process (e.g., approximately 0.5 μm when using 100X magnification power). This limits the optical focal depth of the images. Hence, to acquire the complete FISH signals distributed in a FISH-probed specimen with depth of 4 to 5 μm, the specimen slide needs to be scanned in multiple layers, which generates a huge amount of image data to acquire interphase cells and FISH signals distributed in a three-dimension (3-D) space. Visually examining and analyzing such huge amount of 3-D image data is not feasible in clinical practice. To overcome this disadvantage, we investigated in this study how to automatically and effectively search for and select the limited image data that depict analyzable interphase cells by discarding the majority of un-useful or redundant data as well as to convert 3-D image visualization into a more efficient and reliable 2-D image analysis. For this purpose, we developed and tested a computer-aided detection (CAD) scheme to preprocess the automated images acquired using a prototype dual-detector based fluorescence image scanning system by detecting the analyzable interphase cells and mapping the related stack of 3-D image slices into a 2-D projection or fused image. The CAD scheme continued to detect and count FISH-probed chromosome signals. By comparing the automated FISH signal detection result with the independent visual detection result of an experienced observer, we assess the feasibility of our automated method to assist FISH signal analysis under a high-resolution image scanning mode.

2. Materials and method

2.1. A new automated FISH image scanning system

Unlike the existing single detector based FISH image scanning systems that are required to scan FISH specimen multiple times by changing the spectrum filters to acquire the multiple spectrum signals, we developed a multi-spectral prototype FISH imaging analysis system that enables to acquire two fluorescent spectrum images containing the interphase nuclei and FISH-probed chromosome signal in two different spectrum simultaneously by two detectors using the optical concept described elsewhere [23]. In brief, this automatic dual-detector based FISH prototyping imaging system was built using a Nikon eclipse 50i microscope as a platform by adding two monotonous digital (CCD) detectors connected with a frame grabber and a motorized scanning stage. Specifically, the microscope contains a 100 W mercury lamp with main emitted wavelengths at 365, 400, 440, 546, and 580 nm, a collector lens to convert the illuminated light beam into the parallel beam, the neutral density filters to minimize the process of quick photobleaching, and the optic components that include objective lens (e.g. 100X objective lens with numerical aperture of 1.25), multiple excitation, emission, and dichroic filters to acquire images of FISH signals distributed in different spectrum. To acquire high quality and resolution images, each CCD detector has 1392×1040 pixel array with pixel size of 6.45×6.45 μm. The average quantum efficiency of the detector reaches 0.8 at spectrum from 400 to 700 nm. Using this dual-detector optical system, the fluorescence emissions of cell nuclei (e.g., in blue color) and single FISH-probe signal (e.g., in green color) from specimen is separated by dichroic filters and acquired by two detectors, respectively. Meanwhile, a motorized scanning stage driven by a high precision stepping motor is able to reaches 1 μm resolution in lateral directions and 0.1 μm resolution in axial direction.

2.2. An image dataset

In this study we selected four Pap-smear specimen slides acquired from four women underwent the cervical cancer screening examinations in the University of Oklahoma Health Sciences Center. Studies have identified that the trisomy of three chromosomes (3, 7, and X) had significant impact in cervical cancer development and prognosis [24–27], we applied the following method to process the acquired specimen slides. The interphace cell nuclei were counterstained by Vectashield (Vector Laboratories, Burlingame, CA) containing 0.5 μg/ml 6-diamidino-2-phenylindole (DAPI), which can be captured in the fluorescent blue color (spectrum). Since we used a dual-detector based FISH image scanning system, an

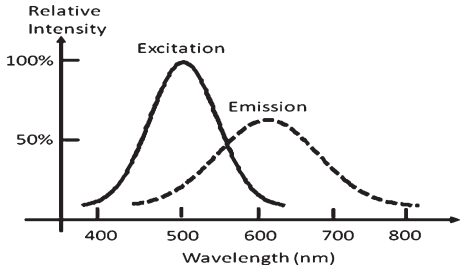

Fig. 1. An example of excitation and emission spectrum for a fluorochrome.

additional fluorochrome in fluorescent green color (spectrum) was applied to probe or dye chromosome X in this study. The fluorochrome emits fluorescent light at a narrow wavelength that can pass the cooperation of specific dichroic filter and barrier filter [28]. Figure 1 describes the typical example of excitation and emission spectrum for a fluorochrome. For this purpose, a centromeric CEP X (DXZ1) spectrum green probe (manufactured by Vysis, Abbott Molecular Inc., Downers Grove, IL) was applied to process the acquired each Pap-smear specimen slide using a standard FISH probing procedure that includes the steps of pretreatment, denature, hybridization, and post-hybridization to produce FISH labeled biomarker slides from the originally acquired specimen of Pap-smear examinations [29]. After processing with the designated FISH signal probes, each FISH-probed specimen slide was then automatically scanned using our dual-detector fluorescent image scanning system to acquire two separated sets of image stacks containing the interphase cells in blue spectrum and FISH-probed chromosome X signals in green spectrum simultaneously. A normal cell should include two FISH-probed signal spots, while the cells including only one or more than two FISH signal spots are abnormal cells. Figure 2 shows an example of a normal cell with two chromosomes X (a) and two abnormal cells with one chromosome X (b) and three chromosomes X (c) which are automatically scanned and captured by a monochromatic image detector passing through green spectrum filter.

When using this dual-detector based microscopic FISH image scanning system with a 100X microscopic objective lens to scan a FISH-probed specimen slide, the field depth of each scanned image slice is limited to approximately 0.5 μm. Since FISH-probed specimen typically has 4 to 5 μm thickness, some FISH signals distributed in the 3-D space may be out of focus in one image scanning. Hence, the FISH-probed specimen slide was scanned in nine contiguous slices (without space gap between two slices), which generates the stacks of nine image slices to record 3-D FISH signal information. The image data of approximately 32GB was produced for scanning each FISH probed specimen slide. In each location (x, y) parallel to the surface of FISH-probed specimen slide, two sets of image stacks (slides) are generated. One set records the interphase cell nuclei and one set images the FISH-probed chromosome X signals.

2.3. A computerized scheme

The scanned image data was automated processed by a CAD scheme to detect the volumes of interest (VOIs) that contain the potentially analyzable interphase cells. A sharpest cell image is selected from nine image frames in the blue spectrum and the stack of image slides containing FISH-probed signals is mapped into this selected cell image slide to generate a 2-D projection image. The CAD scheme is then applied to the mapped 2-D projection images to detect FISH-probed signals. For this purpose, our CAD scheme includes the following steps.

1. **Generating the combined 2-D projection image.** Unlike a FISH-probed chromosome signal that may only be recorded in a few of nine image slices due to its small size, an interphase cell nuclei is much bigger in size and can be recorded in all of image slices with blurring boundary in some slices due to effect of out-focusing. Hence, in the stack of images recording the interphase cells, the CAD scheme is first applied to detect and select one image slice with the sharpest cell boundary to detect potentially analyzable cells. Figure 3 illustrates an example of region of interests (ROIs) containing an interphase cell in blue spectrum (Fig. 3a–i). After capturing the image stack of nine image slices, CAD scheme was applied to search for the best focused FISH image. Specifically, a digital derivative filter [30] was applied in the x direction of scanned FISH signal images. The focus energy or sharpness index (SI) of the image is computed as:

$$F_{best} = MAX(F(z)) = \log\left(\sum_{x=1,y=1}^{x=M,y=N} (I(x+1, y, z) - I(x-1, y, z))^2\right), \quad z = 1, ..., 7, \qquad (1)$$

Fig. 2. An example of a normal cell with two chromosomes X (a), two abnormal cells with one chromosome X (b), and three chromosomes X (c) automatically scanned and obtained in green fluorescent spectrum.

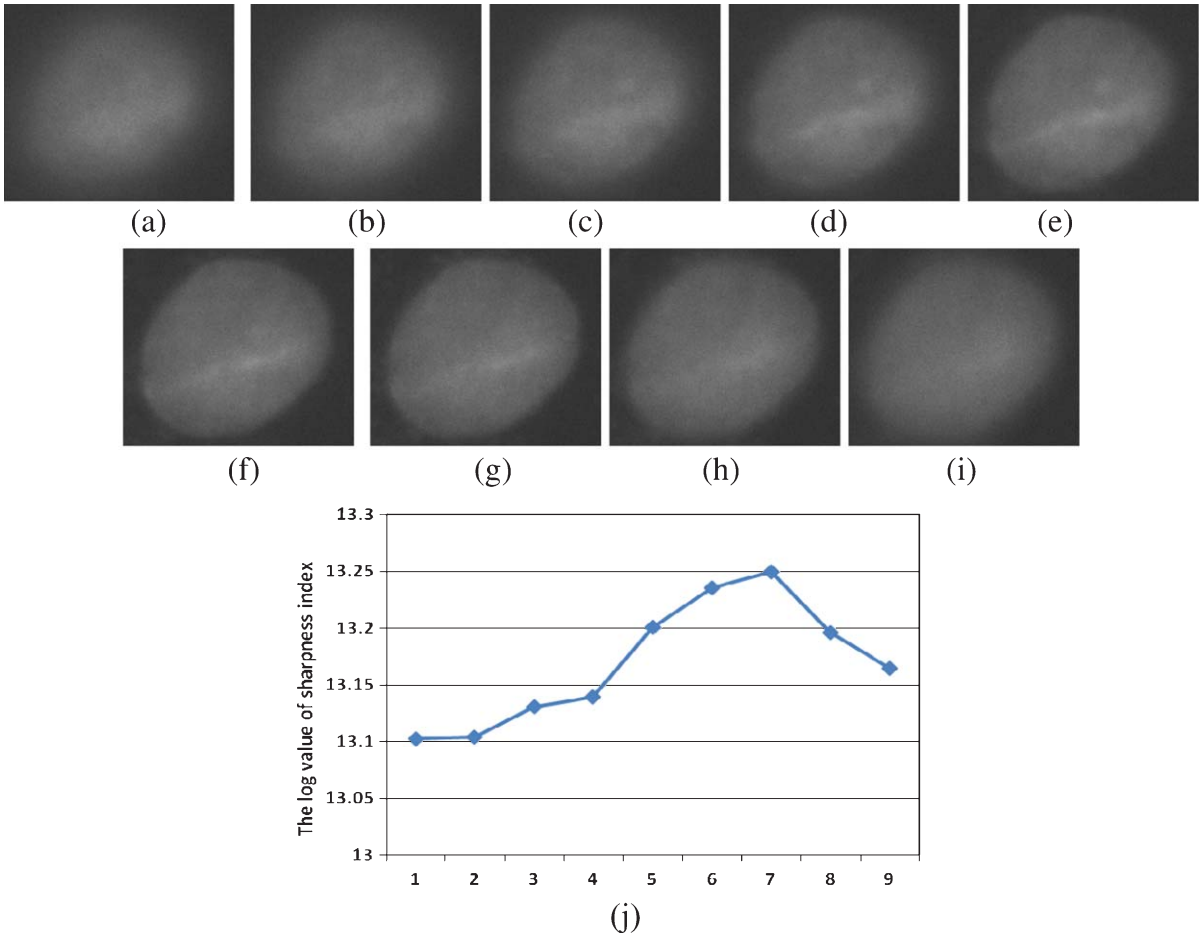

Fig. 3. An example of a stack of cell image slices captured in the first cell-targeted spectrum in nine focal planes (from (a) to (i)) and the change of the computed sharpness indices from these nine cell image slices.

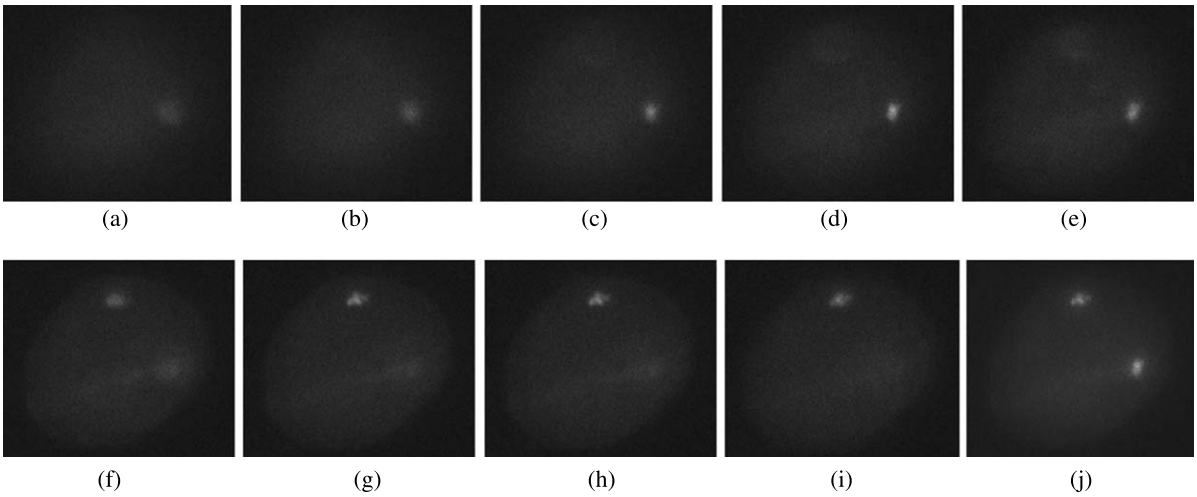

Fig. 4. An example of a stack of FISH signal image slices captured in the second FISH signal targeted spectrum in 9 focal planes (from (a) to (i)) and an integrated 2-D projection image (j) by the MIP method.

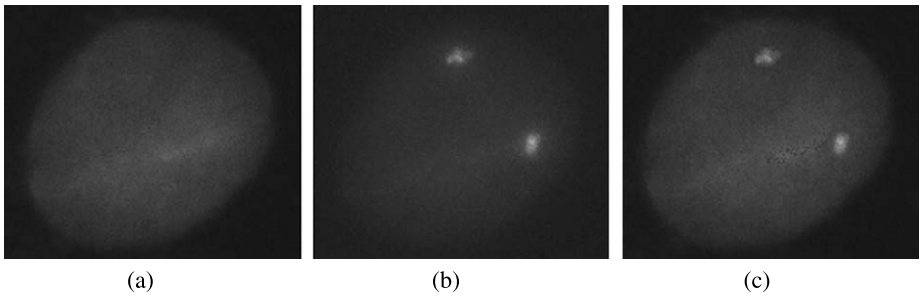

Fig. 5. An example of an integrated fusion image (c) obtained from the sharpest cell image in the first cell targeted spectrum (a) and a 2-D projection image (b) obtained from in the second FISH signal targeted spectrum.

where the size of image I is $M \times N$, and F_{best} represents the sharpest image in the optimal focus. Thus, the image slice with maximum F value in multiple images of one cell was selected. Figure 3j compares the sharpness index computed from 9 scanned image slices as shown in Fig. 3a–i. In this example, CAD selected the seventh image frame (Fig. 3g) as the best focused FISH image that is also consistent with the visual selection. Once a cell candidate is detected and segmented, a classifier based on criteria of region size and circularity [31] is applied to identify or classify whether this candidate represents an analyzable cell or un-analyzable object (i.e., debris or clustered cells). Then, the CAD scheme uses the (x, y) coordinate of the detected cell center and cell boundary in the ROI to define a volume of interest (VOI) in another image stack that records the FISH-probed chromosome signals. All FISH-probed signal spots recorded in the multiple image slices (in z direction) are mapped into cell ROI using a maximum intensity projection (MIP) method that enables to map a stack of 3-D image slices into one 2-D projection image [32]. Figure 4 illustrates an example of region of interests (ROIs) containing FISH signal spots captured in green spectrum in 9 focal planes (Fig. 4a–i). Due to the limited focusing depth, the two FISH-probed signal spots are distributed in different focus planes. One spot are captured in Fig. 4a–e with different degree of blurring, while another spot appears in Fig. 4f–i. Using the MIP method, these two FISH-probed signal spots were mapped into one 2-D projection image or pre-detected interphase cell as shown in Fig. 4j. As a result, once a cell is detected, two sets of image stacks (with a total of 18 image frames in this experiment) is converted into one 2-D projection image that preserves

the cell morphology and all FISH-probed signal spots depicted inside the cell. In summary, Fig. 5 shows the integrated fusion images based on the sharpness index and the MIP method.

2. **Image processing using the full-scale contrast stretching and a Gaussian filter.** After generating the 2-D projection ROIs containing the analyzable cells and the mapped FISH-probed signal spots, these ROIs can be combined into one 2-D projection image, $I(x, y)$. This image is processed aiming to improve signal-to-noise level of the recorded interphase cell or nuclei and in particular the recorded FISH-probed chromosome signals using two steps. First, the images is converted into a new image, $I'(x, y)$, by a full-scale contrast stretching method:

$$I'(x, y) = 255/(I_{\max}(x, y) - I_{\min}(x, y)) * (I(x, y) - I_{\min}(x, y)) \quad (2)$$

Then, a Gaussian filter is applied on both horizontal and vertical directions, respectively, to further reduce image noise. The processed 2-D FISH image can then be examined or analyzed by either the observers (e.g., the cytogenetic laboratory technicians or cytogeneticists) or our CAD scheme to detect or count the FISH-probed chromosome signal spots.

3. **Detecting and segmenting interphase cell nuclei.** When using CAD scheme to detect FISH signal spots, the scheme first detects and segments the interphase cell nuclei. Due to the uncontrollable technical issues in the specimen slide preparation including the FISH probing process, the intensity levels of different interphase cell nuclei depicted on the image often have different intensity distributions [33]. Instead of a fixed simple threshold that often cannot segment all analyzable interphase cells, the CAD scheme applies an iterative multiple-threshold approach to detect and segment the varies of analyzable interphase cells depicted on the projected image [2]. After initial segmentation of suspicious interphase cell nuclei, a morphological opening filter with a 5×5 square kernel is applied to separate adjacent ("touching" or connected) areas and delete small isolated areas. By analyzing the size, compactness, radial length, circularity of each candidate, the scheme is able to delete the overlapped cells, clusters, and other noisy debris, while preserving the analyzable interphase cells.

4. **Detecting and segmenting FISH-probed signal spots.** CAD scheme then detects and segments the FISH-probed chromosome signal spots located inside the detected/segmented interphase cell nuclei. For this purpose, a top-hat transform algorithm [16] is applied to detect and segment the FISH-probed signal spots (or biomarkers). The method can be described as:

$$top\text{-}hat\,(f, B) = f - f \circ B \quad (3)$$

where f represent the originally acquired FISH-probed signal image, B is a square structure with 7×7 window (kernel) size, and $\circ$ is the morphological opening operator.

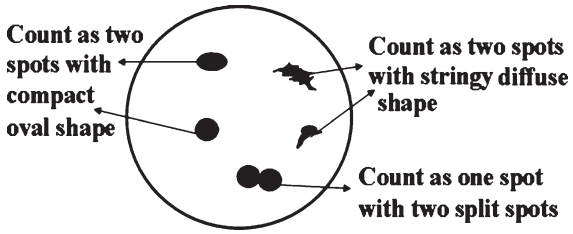

Fig. 6. Examples of stringy, splitting, and typical FISH spots.

5. **Counting independent FISH-probed signal spots using a knowledge-based classifier.** Due to the characteristics of the centromeric enumeration probe CEPX, most of FISH labeled signals used to target chromosomes X are stringy and splitting as illustrated in Fig. 6. To avoid automated counting errors, a knowledge-based classifier developed in our previous study [33] is used in the CAD scheme to identify and merge the splitting and stringy FISH spots. In brief, this is a decision-tree type classifier that includes six image features (or nodes) related to the average or relative pixel value (intensity) inside one FISH spot, the size and shape factor of the FISH spot, and the distance between the two nearest neighbor FISH spots in the same fluorescent spectrum. CAD scheme can then count number of FISH-probed signal spots depicted inside each detected/segmented interphase cell.

2.4. CAD performance assessment

To make automated FISH image and signal analysis eventually clinically useful, CAD scheme must have a high performance level in accurately counting FISH-probed signal spots and compute the ratio between the normal and/or abnormal cells. To assess CAD performance, we in this study also asked one observer (an experienced cyto-genetic laboratory technician) to visually detect and count the FISH signal

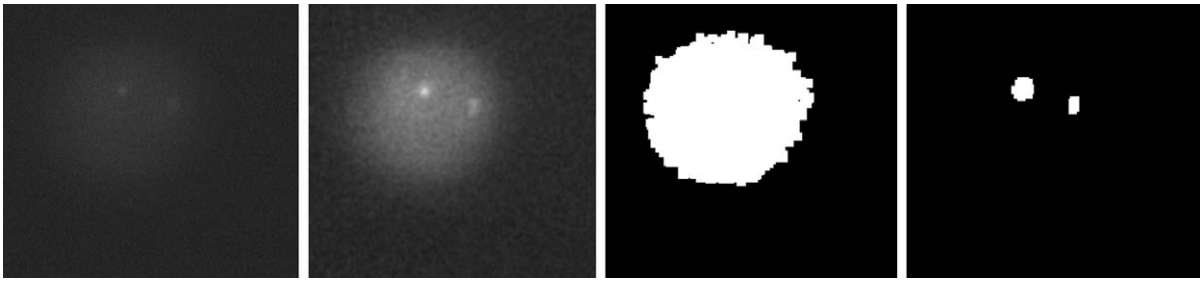

(a) (b) (c) (d)

Fig. 7. (a) The ROI containing a potential FISH cell; (b) the pre-processed image through the full-scale contrast stretching and Gaussian filter; (c) the segmented FISH cell by the adjustable threshold algorithm and morphologic processing; (d) The segmented FISH signals by top-hat algorithm and morphologic processing.

Table 1
The CAD analyzing results of FISH signals on con-focal images

Case number	Chromosome X			Total cells
	1	2	>2	
1	146 (59.8%)	68 (27.9%)	30 (12.3%)	244
2	145 (63.9%)	60 (26.4%)	22 (9.7%)	227
3	43 (28.1%)	85 (55.6%)	25 (16.3%)	153
4	252 (72.6%)	40 (11.5%)	55 (15.9%)	347

Table 2
The technician analyzing results of FISH signals on con-focal images

Case number	Chromosome X			Total cells
	1	2	>2	
1	133 (54.5%)	94 (38.5%)	17 (7.0%)	244
2	134 (59%)	76 (33.5%)	17 (7.5%)	227
3	26 (17.0%)	102 (66.7%)	25 (16.3%)	153
4	250 (72.0%)	36 (10.4%)	61 (17.6%)	347

spots depicted on all analyzable cells detected by our CAD scheme. The Kappa coefficient for agreement between the automated (CAD) and visual (an observer) detection results was computed as a summary index to assess CAD performance in detecting independent FISH signal spots and classifying between normal and abnormal cells. The experimental and data analysis results are tabulated and compared.

3. Results

CAD scheme was able to detect 244, 227, 153, and 347 potentially analyzable interphase cells recorded in the image stacks of four testing specimens, respectively. Around these detected cells in each case, CAD scheme generated the final 2-D projection image by mapping all corresponding FISH-probed signal spots on the image. The 2-D projection images were considered acceptable by both observer and CAD scheme in further detecting and counting FISH-probed signal spots inside the detected and segmented analyzable interphase cells. Figure 7 shows an example of applying the CAD scheme to detect FISH-probed signal spots from a detected/segmented cell in which the original ROI of the cell, the processed cell using the full-scale contrast stretching method and Gaussian filter, as well as the finally detected/segmented cell and the detected/counted FISH-probed signal spots, are demonstrated.

Table 3
The computed Kappa coefficients for agreement between the CAD scheme and the observer in analyzing the four testing cases

Case number	Kappa coefficients		
	1	2	>2
1	0.891	0.765	0.696
2	0.897	0.833	0.859
3	0.687	0.771	1.000
4	0.985	0.940	0.937

Tables 1 and 2 summarize and compare the number of the detected interphase cells that include one, two, or more than two FISH-probed signal spots (representing the number of chromosome X) detected and counted by the CAD scheme and the observer, respectively. Both CAD and observer identified (counted) more abnormal cells (with only one or more than two FISH-probed

signal spots) than the normal cells (involving only two FISH-probed signal spots) in cases 1, 2, and 4, which indicate that these are highly suspicious cases. The majority cells were counted as normal in case 3 by both CAD scheme and observer. Although the ratios between the normal and abnormal cells in each case computed by the observer and the CAD scheme are different, the trends of the suspicious level for cervical cancer among these four testing cases are the same from both the observer and the CAD assessment results. Table 3 summarizes and compares the computed Kappa coefficients for agreement between the CAD scheme and the observer in analyzing these four testing cases. The experimental results showed the relatively higher agreements of the computed Kappa coefficients ranging from 0.69 to 1.0.

4. Discussion

Although the interphase based FISH technology or test has been well recognized as one of the most powerful and reliable molecular imaging biomarkers or diagnostic tools in diagnosing cancer, assessing its prognosis, and determining the optimal treatment strategies, the currently used manual FISH signal detection and analysis using a fluorescent microscope severely limits its clinical utility. For example, random selection of a limited number of cells and tendency of observers towards the selection of cells with good morphology generates the inevitable bias that may not only reduce the diagnostic sensitivity but also make it very difficult to correctly predict disease prognosis and/or detect residual disease in response to the therapy, which requires counting FISH signals depicting on much large number (if not all) of cells depicted on the targeted specimen slides in the heterogeneous cases [13]. In order to improve the application feasibility of FISH tests, a number of automated FISH image scanning systems with either one or more detectors have been developed and tested. However, to adequately acquire visually detectable FISH-probed signal spots, the automated FISH image scanning system generates a huge amount or stack of image data to produce the high-resolution images. Among them only a fraction of image data actually contains the useful information (or analyzable interphase cells). It is also impractical to conduct visual processing or sorting such huge image data in the busy clinical environment. The unique characteristic or contribution of this preliminary study is that we demonstrated the feasibility of developing and applying a CAD scheme to automatically select useful image data and convert (or map) the multiple 3-D image slices into a single 2-D projection image. This process compresses the huge amount of 3-D image data into the limited and manageable 2-D image data by eliminating a large number of un-useful and redundant image data. The study results show that the automated generated 2-D projection images are not only easy to be visually analyzed/interpreted by the observers (e.g., the cyto-geneticists) and can also be further processed by conventional CAD schemes to detect the FISH-probed signals and compute the ratios between the normal and abnormal cells. The experiment results showed that our automated approach (including the integration of a dual-detector based fluorescent image scanning system and CAD scheme) could effectively and efficiently capture FISH signals distributed in different focus planes (or image slices) and automatically detect the numerical changes of FISH-probed chromosome X with high consistency or agreement with visual examinations.

Although only the Pap-smear specimen slides acquired from cervical cancer screening and detection were selected and tested in this preliminary study, the automated FISH image and signal analysis concept and the CAD scheme presented here are not limited to the Pap-smear specimen only. This CAD scheme can also be easily modified to make it applicable to the other automated FISH image and signal analysis tasks for detecting and diagnosing different cancers or genetic disorders using other types of specimens (i.e., fine needle aspirates, effusion, urine, peripheral blood, and bone marrow). However, despite the encouraging results, this is a very preliminary study with several limitations including (1) the small number of testing specimen slides and (2) the dual-channel fluorescent signals (one for interphase cell and one for FISH-probed chromosome X). Hence, the performance and robustness of this CAD-guided automated image mapping and FISH signal detection approach needs to be further tested in the future studies using more large and diverse FISH-probed specimens. If successful, this automated FISH image generation and signal detection/analysis approach could eventually help significantly enhance the clinical utility of FISH tests to assist clinicians improving the efficiency and accuracy of cancer detection/diagnosis and its prognosis assessment.

Acknowledgment

This research is supported in part by the grants CA115320 and CA136700 from the National Cancer Institute, National Institutes of Health. The authors would like to acknowledge the support of Charles and Jean Smith Chair endowment fund as well. *X Chen is currently with Tianjin University, Tianjin, China.

References

[1] F. Jiang and R.L. Katz, Use of interphase fluorescence *in situ* hybridization as a powerful diagnostic tool in cytology, *Diagnostic Molecular Pathology* **11** (2002), 47–57.

[2] X. Wang, B. Zheng, R.R. Zhang, S. Li, J.J. Mulvihill, X. Lu, et al., Automated analysis of fluorescent *in situ* hybridization (FISH) labeled genetic biomarkers in assisting cervical cancer diagnosis, *Technology in Cancer Research and Treatment* **9** (2010), 231–242.

[3] H. Vrolijk, W.C.R. Sloos, F.M. van de Rijke, W.E. Mesker, H. Netten, I.T. Young, et al., Automation of spot counting in interphase cytogenetics using brightfield microscopy, *Cytometry* **24** (1996), 158–166.

[4] M.C. Cox, P. Panetta, A. Venditti and G.D. Poeta, Comparison between conventional banding analysis and FISH screening with an AML specific set of probes in 260 patients, *Hematol J* **4** (2003), 263–270.

[5] Y. Gong, D.J. Booser and N. Sneige, Comparison of HER-2 status determined by fluorescence *in situ* hybridization in primary and metastatic breast carcinoma, *Cancer* **103** (2005), 1763–1769.

[6] H. Mark, D. Mills, K. Santoro, M. Quddus and J. Lathrop, Fluorescent *in situ* hybridization analysis of cervical smears, A pilot study of 20 cases, *Annals of Clinical and Laboratory Science* **27** (1997), 224–229.

[7] I.A. Sokolova, L. Bubendorf, A. O'Hare, et al., A fluorescence *in situ* hybridization-based assay for improved detection of lung cancer cells in bronchial washing specimens, *Cancer* **96** (2002), 306–315.

[8] M. Marin-Aguilera, L. Mengual, M. Ribal, et al., Utility of a multiprobe fluorescence *in situ* hybridization assay in the detection of superficial urothelial bladder cancer, *Cancer Genetics and Cytogenetics* **173** (2007), 131–135.

[9] T. Haferlach, W. Kern and S. Schnittger, Modern diagnostics in acute leukemia, *Crit Rev Oncol Hematol* **56** (2005), 223–234.

[10] A.C. Wolff, M. Hammond, J.N. Schwartz, et al., American Society of Clinical Oncology/College of American Pathologists guideline recommendations for human epidermal growth factor receptor 2 testing in breast cancer, *Archives of Pathology and Laboratory Medicine Online* **131** (2007), 18–43.

[11] Network NCC. Chronic mylogenous leukemia clinical practice guidelines in oncology. http://www.nccn.org.; 2008

[12] S. Paik, J. Bryant, E. Tan-Chiu, E. Romond, W. Hiller, K. Park, et al., Real-world performance of HER2 testing–National surgical adjuvant breast and bowel project experience, *Journal of the National Cancer Institute* **94** (2002), 852–854.

[13] G.A. Dewald, W.A. Wyatt and A.L. Juneau, Highly sensitive fluorescence *in situ* hybridization method to detect double BCR/ABL fusion and monitor response to therapy in chronic myeloid leukemia, *Blood* **91** (1998), 3357–3365.

[14] K.C. Halling, W. King and I.A. Sokolova, A comparison of cytology and fluorescence *in situ* hybridization for the detection of urothelial carcinoma, *J Urol* **164** (2000), 1768–1775.

[15] A.D. Carothers, Counting, measuring and mapping in FISH-labeled cells: Sample size considerations and applications for automation, *Cytometry* **16** (1994), 298–304.

[16] H. Netten, I.T. Young, L.J. Vliet, H.J. Tanke, H. Vroljik and W.C.R. Sloos, FISH and chips: Automation of fluorescent dot counting in interphase cell nuclei, *Cytometry* **28** (1997), 1–10.

[17] B. Lerner, W.F. Clocksin, S. Dhanjal, M.A. Hulten and C.M. Bishop, Automatic signal classification in fluorescence *in situ* hybridization images, *Cytometry* **43** (2001), 87–93.

[18] R. Malka and B. Lerner, Classification of fluorescence *in situ* hybridization images using belief networks, *Pattern Recognition Letters* **25** (2004), 1777–1785.

[19] N. Malpica, C.O. de Solórzano, J.J. Vaquero, A. Santos, I. Vallcorba, J.M. García-Sagredo, et al., Applying watershed algorithms to the segmentation of clustered nuclei, *Cytometry* **28** (1997), 289–297.

[20] T.W. Ridler and S. Calvard, Picture thresholding using an iterative selection method, *IEEE Trans Systems, Man and Cybernetics* **8** (1978), 630–632.

[21] Z. Li, S. Li, B. Zheng, R. Zhang, Y. Li, H. Tian, W. Chen and H. Liu, Potential clinical impact of 3-D visualization for fluorescent *in situ* hybridization (FISH) image analysis, *J Biomed Optics* **17** (2012), 050501.

[22] Martin De Biasio, Enhancement of m-FISH images using spectral unmixing, *International Journal of Biological and Life Sciences* **3**(4) (2007), 231–237.

[23] X. Chen, B. Zheng and H. Liu, Optical and digital microscopic imaging techniques and applications in pathology, *Analytical Cellular Pathology* **34** (2011), 5–18.

[24] C. Sreekantaiah, M.D. Braekelee and O. Haas, Cytogenetic findings in cervical carcinoma. A statistical approach, *Cancer Genetics and Cytogenetics* **53** (1991), 75–81.

[25] C. Mian, D. Bancher, P. Kohlberger, C. Kainz, A. Haitel, K. Czerwenka, et al., Fluorescence *in situ* hybridization in cervical smears: Detection of numerical aberrations of chromosomes 7, 3, and X and relationship to HPV Infection, *Gynecologic Oncology* **75** (1999), 41–46.

[26] P. Segers, S. Haesen, P. Castelain, J.J. Amy, P.D. Sutter, P.V. Dam, et al., Study of numerical aberrations of chromosome 1 by fluorescent *in situ* hybridization and DNA content by densitometric analysis on (pre)-malignant cervical lesions, *The Histochemical Journal* **7** (1995), 24–34.

[27] K. Heselmeyer-Haddad, K. Sommerfeld, N.M. White, N. Chaudhri, L.E. Morrison, N. Palanisamy, et al., Genomic amplification of the human telomerase gene (TERC) in pap smears predicts the development of cervical cancer, *American Journal of Pathology* **166** (2005), 1229–1238.

[28] M. Müller, Introduction to confocal fluorescence microscopy: SPIE Press; 2005.

[29] X. Wang, B. Zheng, R.R. Zhang, S. Li, J.J. Mulvihill, X. Lu, et al., Automated analysis of fluorescent *in situ* hybridization (FISH) labeled genetic biomarkers in assisting cervical cancer diagnosis, *Technology in Cancer and Treatment* **9** (2009), 231–242.

[30] F.R. Boddeke, L.J.V. Vliet, H. Netten and I.T. Young, Autofocusing in microscopy based on the OTF and sampling, *Bioimaging* **2** (1994), 193–203.

[31] B. Zheng, J.K. Leader, G.S. Abrams, A.H. Lu, L.P. Wallace, G.S. Maitz, et al., Multiview-based computer-aided detection scheme for breast masses, *Med Phys* **33** (2006), 3135–3143.

[32] X.H. Wang, J.E. Durick and A. Lu, Characterization of radiologists' search strategies for lung nodule detection: Slice-based versus volumetric display, *J Digit Imaging* **21** (2008), S39–S49.

[33] X. Wang, B. Zheng, S. Li, R. Zhang, J.J. Mulvihill, W.R. Chen, et al., Automated detection and analysis of fluorescent *in situ* hybridization (FISH) spots depicted in digital microscopic images of pap-smear specimens, *Journal of Biomedical Optics* **14** (2009), 1–10.